

Four-center energy transfer and interaction pairs: Molecular quantum electrostatics

Robert D. Jenkins^{a)} and David L. Andrews^{b)}

School of Chemical Sciences, University of East Anglia, Norwich, NR4 7TJ, United Kingdom

(Received 16 October 2001; accepted 24 January 2002)

In the photophysics of complex macromolecules, resonance energy transfer is the key mechanism for the migration of electronic excitation. As the ability to engineer specific architectures for such molecules improves, environments for new forms of energy migration are being envisioned. Set in this context, one of our aims in this paper is to expound a new, general way of representing complex energy transfer systems, to obviate semantic and conceptual problems in addressing multicenter interactions. The theory of four-center energy transfer is developed within this framework, through the application of molecular quantum electrostatics. A variety of mechanisms is identified by which four-center energy transfer may proceed, and a recently developed diagrammatic technique is employed to calculate relevant quantum amplitudes. Symmetry considerations are addressed, and key features of the ensuing rate equations are discussed with regard to their potential exploitation in novel photoactive devices. © 2002 American Institute of Physics. [DOI: 10.1063/1.1461820]

I. INTRODUCTION

In recent years the increasingly sophisticated design and synthesis of multi-chromophore macromolecules has led to the need for a better understanding of the interplay between their electronic and optical properties. The need is keenest in the area of nanoscale photoactive materials, ranging from dendrimers to multiporphyrin macromolecules. The most advanced of these multichromophore systems hold considerable technological promise for biomimetic energy conversion.¹ Indeed, skilled synthetic manipulation of nanoscale environments has produced molecules that prove valuable for modelling the photophysical processes of photonic trapping and migration within the native photosynthetic unit (PSU). It is the movement of energy within such macromolecules that concerns us in this work—particularly with regard to their behavior at high levels of input radiation.

To rationalize recent developments in the transfer of electronic excitation in multichromophore array science it is helpful to look briefly at the development of this subject area. The photophysical mechanism underlying resonance energy transfer (RET), the fundamental hopping process whereby excitation localized at one chromophore migrates to another, is well understood in both theory and practice.² Early studies focused on bichromophore molecules,^{3,4} the component chromophores being either chemically identical^{5,6} or different.⁷ The critical effect of bridging species interposed between the two units was soon appreciated.^{8,9} As structural linkages, such bridges can impart either rigidity or flexibility, and numerous studies have been undertaken on each variety—see, for example, Refs. 10 and 11. More recent investigations have centered on the modeling and analysis of multichromophore arrays^{12,13} as a focus of synthetic effort towards an efficient mimic of the

PSU.^{14–16} Utilizing fluorescence resonance energy transfer,^{17,18} spectroscopic techniques applied to a variety of the above systems have given information such as transfer rates, interchromophore separations^{19,20} and the orientations of transition dipoles.²¹ Recent work has identified such systems as possible components in molecular logic gates.²²

The onset of dendrimer chemistry in the 1990's opened further avenues of investigation. Dendrimeric macromolecules can be viewed as multibranching systems of interconnected chromophores, conceptually akin to multiporphyrin arrays. Physically they comprise photoactive dendrons which trap energy and channel it, via energy transfer hops, towards a central core. As such they are ideal for modeling light-harvesting proteins,^{23,24} since direct parallels can be drawn with the roles of chlorophyll and the reaction center in the PSU. In dendrimeric macromolecules, both the central core and branch chromophores may be manipulated to display a variety of optical and architectural properties.^{25,26} It is the exploitation of these traits that stimulates the pursuit of recently proposed high-intensity phenomena such as three-center energy transfer (3CET, *vide infra*), with encouraging results already published.^{27,28}

This paper is set out as follows: First we describe RET in terms of a new concept, the interaction-pair. The technique is extended to more complex three-center systems. In the remainder of the paper we focus on the process of four-center energy transfer (4CET). A variety of mechanisms and permutations by which 4CET may occur are described using terminology previously developed for the three-center analog (3CET). By application of a new technique involving state-sequence diagrams, the quantum amplitudes of 4CET are calculated. We conclude this work with a discussion on the symmetry aspects of systems which may display 4CET behavior, and suggestions for their implementation.

^{a)}Electronic mail: robert.jenkins@uea.ac.uk

^{b)}Electronic mail: d.l.andrews@uea.ac.uk; fax: +44 (0) 1603 592014.

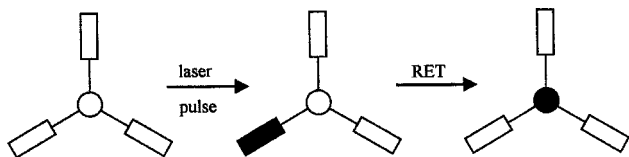


FIG. 1. Idealized dendrimeric system with three-fold symmetry showing the essential photophysics of RET. The molecule is made up of three “dendrons” attached to a trap. Excitation is shown by black shading. An initial laser pulse excites a dendron (or a chromophore therein); energy is then transferred to the core via RET.

II. INTERACTION-PAIRS: RESONANCE ENERGY TRANSFER

A majority of energy migration processes in the systems described above occur between electronically distinct chromophores separated beyond wavefunction overlap, and are fully explicable in terms of resonance energy transfer,²⁹ in regions where wavefunction interaction is strong, transfer is mediated by a direct exchange mechanism.^{30,31} The essence of RET may be illustrated by the nonchemical equation;



which describes the transfer of excitation between a pre-excited donor species A and a ground state acceptor B, their electronic states denoted by superscripts (Greek characters indicate an electronic excited state, 0 the ground state). A pictorial representation of RET in a stylized dendrimeric system is shown in Fig. 1. Note that the excitation is localized at a single branch; for the purposes of this illustration we assume that there is negligible excitonic coupling between branches, and we concentrate upon simple energy transfer between one branch and the core. In the past, RET was conceived as proceeding by one of two mechanisms: in the short-range (tens of angstroms) a radiationless mechanism formulated by Förster,³² obeying an inverse sixth power dependence on inter-species displacement; in the long-range (beyond hundreds of angstroms) a radiative emission-capture mechanism displaying the well-known inverse square dependence.³³ Both pathways have since been shown to be asymptotic limits of a unified theory, which also identifies an intermediate influence with an inverse quartic power dependence.³⁴

In the unified theory of resonance energy transfer the coupling of donor and acceptor transitions is mediated by the propagation of a virtual photon. This cannot be detected without an intervention that completely changes the nature of the process; in this respect the photon plays a similar role to the virtual electronic states involved in scattering processes.³⁵ The virtual photon formalism entails summation over all possible wave vectors and polarizations, just as a virtual molecular state invokes summation over all possible energy levels. At short donor–acceptor separations (those within the normal Förster limits) the photon can be considered purely virtual, but as the pair separates it takes on an increasingly real character until (in the regime of radiative

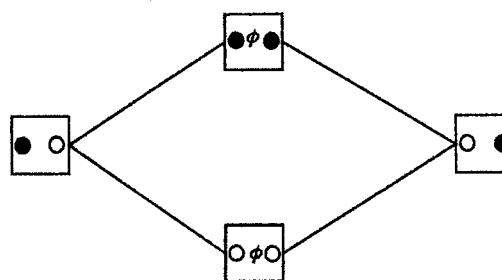


FIG. 2. State sequence diagram for RET. Donor A and acceptor B are represented by circles on the left and right of each box, respectively. Excited state species are shaded black, ground state species are unshaded. The presence of a virtual photon is indicated by ϕ .

transfer) virtual traits become indiscernible. In the unified theory this behavior is seamlessly accommodated into a single, all-encompassing formalism.

In the discussion of the migration of electronic excitation, imprecise usage of language is rife. The problems are often difficult to circumvent, as the simplicity of (2.1) fails to convey the subtlety of the mechanism it describes. Resonance energy transfer is accommodated by the creation and annihilation of a virtual photon and fundamentally entails an interaction of the (vacuum) radiation field with both A and B. The dictates of the time–energy uncertainty principle, coupled with the short photon propagation time, preclude the physically intuitive assumption that the photon creation occurs at A first. Consequently it is necessary to recognize two transfer pathways whose quantum amplitudes must be summed to properly formulate the unified RET description. These transfer pathways can be represented by a state-sequence diagram as shown in Fig. 2. Tracing the lower pathway; the virtual photon is created at the donor A and annihilated at the acceptor B. The upper path depicts the opposite case where the virtual photon is created at B and annihilated at A (see the figure legend). As both paths lead to the same final state, the theory of RET requires a summation of the corresponding quantum amplitudes. Even though the former amplitude associated with the lower pathway becomes dominant as the donor–acceptor separation increases, the latter upper pathway can never be entirely discounted. In this respect, to envisage the photon carrying the excitation “departing” from A and “arriving” at B sanctions an unjustified semantic prejudice—as it excludes the latter mechanism. Moreover when the intricacy of transfer systems increases (by the inclusion of more donors and/or acceptors, *vide infra*), although we still seek a description of the *overall* transfer, it ceases to be correct to ascribe a precise directionality to energy propagation *during* the process, both due to its ultrafast nature and also the accessing of virtual molecular states. Overall transfer generally proceeds by a variety of pathways, the totality of the effect being described by a sum of the corresponding quantum amplitudes.

To circumvent the semantic imprecision identified above, we introduce the concept of an *interaction-pair*. Trivially for resonance energy transfer itself, the interaction-pair is defined by the two species which exchange a virtual photon in the terms laid out above. The interaction-pair is

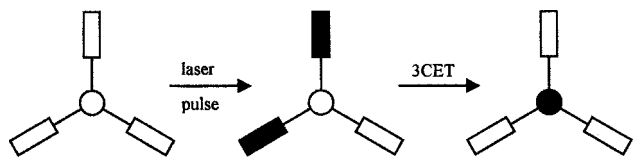
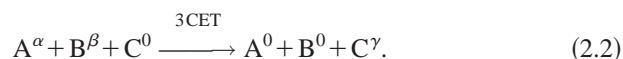


FIG. 3. Idealized dendrimeric system showing the essential photophysics of 3CET.

written and ordered as AB. As neither A nor B accesses virtual molecular states during RET, it is correct to say that, overall, energy is transferred *from A to B*. However by representing the process as AB we recognize *both* the time-orderings involved in the virtual photon exchange enabling the transfer shown in Fig. 2. To this end we anticipate and obviate problems which otherwise arise in complex energy transfer systems.

A. Three-center energy transfer (3CET)

Interaction-pair notation proves its value in more complex, higher order energy transfer processes. Three-center (twin-donor) energy transfer, the subject of a number of recent theoretical works,³⁶⁻⁴³ is described in a similar manner to (2.1) by the nonchemical equation;



The basic photophysics of 3CET are illustrated in Fig. 3. Again we neglect excitonic delocalization, an assumption we revisit in the Discussion, Sec. V. The twin-donor process is known to proceed *via* an amalgam of three mechanisms. First, a *cooperative* mechanism³⁶ may be described as the resultant of the two interaction-pairs AC BC. As before, notation here indicates that electronic excitation energy is transferred between initially excited donors A and B and the acceptor C by two virtual photon couplings; one between A and C, the other between B and C. However both transfers occur *concertedly*, not in a stepwise manner. The experimentally irresolvable simultaneity is manifest in the dual registration of chromophore species C within AC BC, indicating that the acceptor plays a pivotal role in both interaction-pairs. The number of interactions a species is subject to is equal to the number of appearances each species makes in the whole interaction-pair description. If this number exceeds one, the chromophore necessarily accesses virtual electronic states. In the case of C above, its dual appearance denotes a two-photon acceptor transition. Furthermore its positioning as the second species in both pairs AC and BC indicates that the interaction has the symmetry character of two-photon absorption. This is borne out by the quantum amplitude for the cooperative mechanism exhibiting a dependence on a second-rank tensor describing the behavior of C.³⁷

In addition to the cooperative mechanism, three-center energy transfer may also proceed by two *accretive* mechanisms,^{38,39} denoted by the interaction-pairs AB BC and BA AC, respectively. Here B (in the former) and A (in the latter) act as bridging species facilitating the overall 3CET process given in (2.2). The dual presence of B in the former, and A in the latter, indicates a two-photon interaction for B

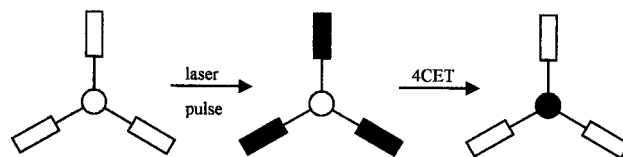
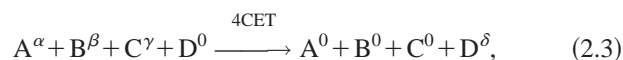


FIG. 4. Idealized dendrimeric system showing the essential photophysics of 4CET.

and A, respectively. Unlike the cooperative mechanism, the species common to both interaction-pairs appear second in one and first in the other. In AB BC for example, B is positioned second in AB and first in BC, such configurations are indicative of the role of B in a scattering-type interaction. Full details of the ensuing quantum electrodynamical calculations are presented elsewhere.^{36-40,42} Recently, general three-center transfer theory has been adapted to account for the effect of a large, nearby static dipole on the rate of RET.⁴⁴

B. Four-center energy transfer (4CET)

Our main focus in this paper is four-center energy transfer. Again in the style of a nonchemical equation, the 4CET interaction may be expressed as



with a cartoon of the process shown in Fig. 4. As in the case of three-center energy transfer described in Sec. II A, no single mechanism adequately describes the overall energy transfer between the four interacting chromophores. Indeed the various couplings which facilitate the interaction give 16 pathways which can be partitioned into four categories (see below). Figure 5 illustrates exemplars of pertinent interaction-pair sets for each 4CET category.⁴² Due to the multitude of processes and pathways involved, 4CET offers the example *par excellence* to illustrate and exploit the interaction-pair concept.

For descriptive purposes, Fig. 5(a) can be identified as a purely cooperative (*coop*) mechanism akin to that seen in three-center energy transfer. The figure depicts the only set of interaction-pairs yielding a *coop* mechanism. Specifically these are AD, BD, and CD with the overall mechanism written as AD BD CD. Here the notation indicates that the quantum amplitude for the *coop* mechanism invokes a three-photon interaction tensor for species D. It is the *coop* mechanism that clearly shows the role of D as a trap, where excitation is exclusively deposited from the donors. Figure 5(b) depicts one of six accretive/cooperative (*acc/coop*)

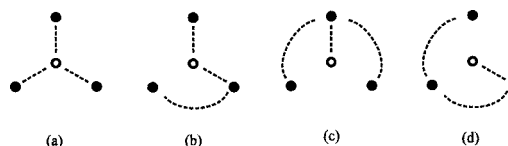


FIG. 5. A depiction of showing interaction-pairs (connected by dotted lines) involved in exemplars of 4CET. The general system comprises the donors ABC (anticlockwise from the top) with acceptor D in the center. Categories are (a) *coop*, (b) *acc/coop*, (c) *coop/acc*, (d) *acc*.

TABLE I. Explicit categories, mechanisms and interaction-pair sets for 4CET. Superscripts denote pictorial representation of mechanism in Fig. 4.

Category	Mechanism	Interaction-pairs
<i>coop</i>	1 ^{4a}	AD BD CD
<i>acc/coop</i>	1 ^{4b}	AD BC CD
	2	AD CB BC
	3	BD AC CD
	4	BD CA AD
	5	CD AB BD
	6	CD BA AD
<i>coop/acc</i>	1 ^{4c}	BA CA AD
	2	AB CB BD
	3	AC BC CD
<i>acc</i>	1 ^{4d}	AB BC CD
	2	CB BA AD
	3	AC CB BD
	4	CA AB BD
	5	BC CA AD
	6	BA AC CD

mechanisms, designated as such since energy moves in an accretive manner between (in this case) interaction-pairs BC and CD, species C adopting the bridging role; concurrently the pairs AD and CD can be conveniently viewed as a cooperative component. Five further *acc/coop* mechanisms may be documented by permuting the two donors in the accretive element interaction-pairs. Continuing, Fig. 5(c) exemplifies one of three cooperative/accretive (*coop/acc*) mechanisms BA CA AD; here BA and CA can be viewed as a cooperative constituent with the AD interaction-pair providing the acceptor excitation. The second and third *coop/acc* mechanisms involve permutation of the species paired with D. Finally Fig. 5(d) signifies a purely accretive (*acc*) mechanism. Here the illustration shows the interaction-pairs BC CA AD, with the other five pathways involving permutation of all three donors. A comprehensive list of categories, mechanisms and interaction-pairs is given in Table I.

III. THEORY OF 4CET

When developing a theory to describe energy transfer mechanisms amenable to multichromophore arrays, and more specifically dendrimers, it is sensible to utilize the framework of molecular quantum electrodynamics (MQED).⁴⁵ Quantum electrodynamics affords a description of the interaction of light and matter in which both are treated quantum mechanically.^{46,47} It is, of course, one of the most successful models in modern physics,⁴⁸ and full quantization of the system constituents distinguishes QED from both fully classical and semiclassical theories. The messenger particle of electromagnetic interactions in QED is the photon, a concept with no analog in semiclassical theory. Phenomena such as spontaneous emission, the Lamb shift⁴⁹ and the Casimir effect^{50–52} can only be satisfactorily explained by QED.⁵³

In dealing with systems comprising slow-moving charges (such as molecules and atoms) the nonrelativistic, noncovariant form of quantum electrodynamics is sufficient.^{54–56} Working in the Coulomb gauge proves advantageous as its representation of a purely transverse electric

field aids the adoption of a multipolar formalism, casting all interactions in terms of the exchange of purely transverse photons.⁵⁷ In the present application, the electric-dipole approximation is made as molecular dimensions are small in comparison with the wave length of the transferred excitation, and all salient transitions are electric-dipole allowed. It is relatively straightforward to accommodate magnetic dipoles, electric quadrupoles and higher order effects of both kinds,⁴⁵ but for our purposes the electric-dipole approximation is sufficient.

The transition amplitude M_{FI} for a system progressing from an initial state $|I\rangle$ to a final state $|F\rangle$ can be described by a time-dependent perturbation theory series expressible as

$$M_{FI} = \langle F | T | I \rangle. \quad (3.1)$$

In Eq. (3.1), T represents the transition operator, explicitly cast as the following expansion in the interaction Hamiltonian H_{int} :

$$T = H_{\text{int}} + H_{\text{int}} \sum_{R_1} \frac{|R_1\rangle\langle R_1|}{E_I - E_{R_1}} H_{\text{int}} + H_{\text{int}} \sum_{R_1} \frac{|R_1\rangle\langle R_1|}{E_I - E_{R_1}} H_{\text{int}} \sum_{R_2} \frac{|R_2\rangle\langle R_2|}{E_I - E_{R_2}} H_{\text{int}} + \dots \quad (3.2)$$

Here $|R_m\rangle$ represent virtual states summed over a complete basis set and denominator terms E_N denote the unperturbed energy of system state $|N\rangle$. In the Coulomb gauge, the quantum electrodynamical interaction Hamiltonian⁴⁵ is a linear sum of the interaction Hamiltonians H_{int}^ξ for all neutral, electronically distinct species ξ in the system. Thus

$$H_{\text{int}} = \sum_{\xi} H_{\text{int}}^\xi. \quad (3.3)$$

The coupling of each interaction-pair entails two H_{int}^ξ operations, so that even order terms, $n = 2q$ in (3.2), represent a $(q+1)$ -center energy transfer system. Thus we look to the sixth order term in (3.2) for four-center energy transfer with $\xi = A, B, C, D$. In the electric-dipole approximation,

$$H_{\text{int}}^\xi = -\epsilon_0^{-1} \boldsymbol{\mu}(\xi) \cdot \mathbf{d}^\perp(\mathbf{r}_\xi), \quad (3.4)$$

where $\boldsymbol{\mu}(\xi)$ is the electric-dipole moment operator associated with ξ and $\mathbf{d}^\perp(\mathbf{r}_\xi)$ is the electric displacement field operator at position vector \mathbf{r}_ξ . Each system state $|N\rangle$ comprises matter and radiation parts and is written in full as

$$|N\rangle = |\text{mol}_N\rangle |\text{rad}_N\rangle \equiv |\text{mol}_N; \text{rad}_N\rangle. \quad (3.5)$$

Here, radiation states relate only to virtual photons. On application of (3.4), $\boldsymbol{\mu}(\xi)$ operates upon the matter states embedded within $|N\rangle$ and $\mathbf{d}^\perp(\mathbf{r}_\xi)$ upon the radiation states. Finally, $\mathbf{d}^\perp(\mathbf{r}_\xi)$ is expressible as a mode expansion:

$$\mathbf{d}^\perp(\mathbf{r}_\xi) = i \sum_{\mathbf{k}, \lambda} \left(\frac{\epsilon_0 \hbar c k}{2V} \right)^{1/2} \{ \mathbf{e}^{(\lambda)}(\mathbf{k}) a^{(\lambda)}(\mathbf{k}) e^{i\mathbf{k} \cdot \mathbf{r}_\xi} - \bar{\mathbf{e}}^{(\lambda)}(\mathbf{k}) a^{\dagger(\lambda)}(\mathbf{k}) e^{-i\mathbf{k} \cdot \mathbf{r}_\xi} \}, \quad (3.6)$$

where $\mathbf{e}^{(\lambda)}(\mathbf{k})$ is the polarization vector associated with a photon of wave vector \mathbf{k} and polarization λ , $\bar{\mathbf{e}}^{(\lambda)}(\mathbf{k})$ being its complex conjugate; $a^{(\lambda)}(\mathbf{k})$ and $a^{\dagger(\lambda)}(\mathbf{k})$ are the photon annihilation and creation operators, respectively, and V is an

arbitrary quantization volume. Note that Eq. (3.6) represents the vacuum development of $\mathbf{d}^\perp(\mathbf{r}_\xi)$. Extensive effort has been undertaken to develop a theory that encompasses the electronic effects of any intervening medium.^{58–61} The technique involves *dressing* the coupling virtual photon. As a result the medium-dressed photons (*polaritons*) are quanta of a dynamical sub-system comprising the radiation field and the medium. The formalism is intricate and, in order to clarify the already complex calculations presented here, the vacuum expansion is adopted for both presentational and physical transparency. A straightforward prescriptive approach to the modification required by a polariton formulation is described elsewhere.⁶²

In the calculational implementation of Eq. (3.1) using (3.2), each application of the interaction Hamiltonian (3.4) can be designated an *index* running up to n , the total number of indices involved in any overall interaction. For example in conventional resonance energy transfer $n=2$ (one interaction at each member of the pair). Indeed any interaction-pair necessarily entails two indices for the virtual photon creation and annihilation events. For a calculation of the complete quantum amplitude (3.1), a summation over all possible index permutations (commonly regarded as time-orderings) must be undertaken. The total number of time-orderings for any mechanism, such the energy migration systems under discussion here, is $n!$. For example, RET involves two (2!) time-orderings, evident in Fig. 2. The process next highest in complexity, 3CET, entails the exchange of two virtual photons yielding 4 indices and 24 (4!) time-orderings *per transfer mechanism*. Thus 72 time-orderings are generated, 24 each for the single cooperative and two accretive channels.^{36,37,40} For four-center energy transfer three virtual photons are involved yielding 720 (6!) index permutations per mechanism. As the total number of mechanisms is 16, the total number of time-ordering permutations enlisted by the overall 4CET quantum amplitude is 11520. Due to the sheer number of contributions, the traditional calculational method of representing each index permutation by a time-ordered diagram is inadequate when tackling such a problem.

A solution to this problem is offered by a new diagrammatic technique that involves mapping the indices as orthogonal unit vectors in an n -dimensional hyperspace (n -space).⁶³ In such a representation only the number of *individual* indices has significance; the exact form of each interaction has no importance. For example, photophysical processes such as Raman scattering and resonance energy transfer both occur in 2-space and prove isomorphic, as each entails two distinct matter–radiation field interactions. The mechanisms of four-center energy transfer involve six distinct indices and their permutation is represented by a 6-space network (see Fig. 6). The network is constructed by combinatorial development of six orthogonal unit vectors and takes the form of a six-dimensional hypercube.⁶³ In 6-space, all the 4CET mechanisms are isomorphic with the nonlinear optical process of 6-wave mixing,^{64,65} where all photons are real and there is no frequency degeneracy.

Any single mechanism of four-center energy transfer involves a unique set of three interaction-pairs (see Table I). Each of the six ensuing matter–radiation field interactions

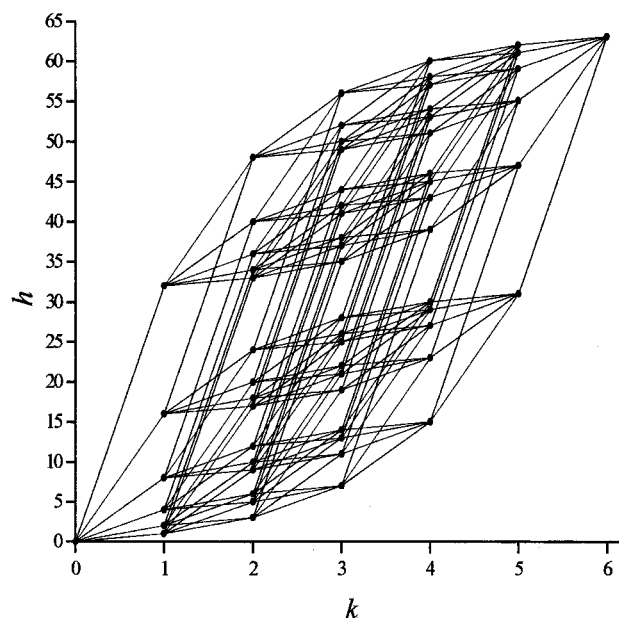


FIG. 6. Hyperspace network mapping the permutation of 6 unique indices. The number of steps k and hyperspace number h (see Ref. 53) are the abscissa and ordinate, respectively.

may be mapped as an index and their permutation described by the 6-space network of Fig. 6. This basic structure forms the blueprint of *state-sequence diagrams*^{36,38,63} (exemplified by Fig. 2) which describe the quantum physics of specific processes. From Eq. (2.2.1) the initial and final states of 4CET are

$$|I\rangle \equiv |r_0^1\rangle = |A^\alpha, B^\beta, C^\gamma, D^0; 0, 0', 0''\rangle \quad (3.7)$$

and

$$|F\rangle \equiv |r_6^1\rangle = |A^0, B^0, C^0, D^\delta; 0, 0', 0''\rangle, \quad (3.8)$$

respectively. Equations (3.7) and (3.8) employ the hyperspace vertex labeling system r_k^m detailed in Ref. 62 and the matter states follow the notation of Eq. (2.1). Naturally, virtual photons are absent from the (real) initial and final radiation states. However, in order to use the same structure for the state vector of intermediate states the potential presence of up to three virtual photons is recognized by including 0, 0' and 0''. When each of the indices which generate Fig. 6 is associated with a fundamental 4CET interaction, each vertex in this figure corresponds to a 4CET system state. The detail of each such state depends on the interaction (index) permutation required to access it. To construct a state-sequence diagram for a specific mechanism is now a matter of writing down all the states accessed, ordered by their connectivity as in Fig. 6. As each 4CET mechanism comprises a different set of fundamental interactions their transposition into 6-space result in unique state-sequence diagrams. In turn each state-sequence diagram embodies 720 time-orderings. Quantum amplitudes given in the following sections have been obtained by explicit identification and summation of all valid paths through these diagrams.

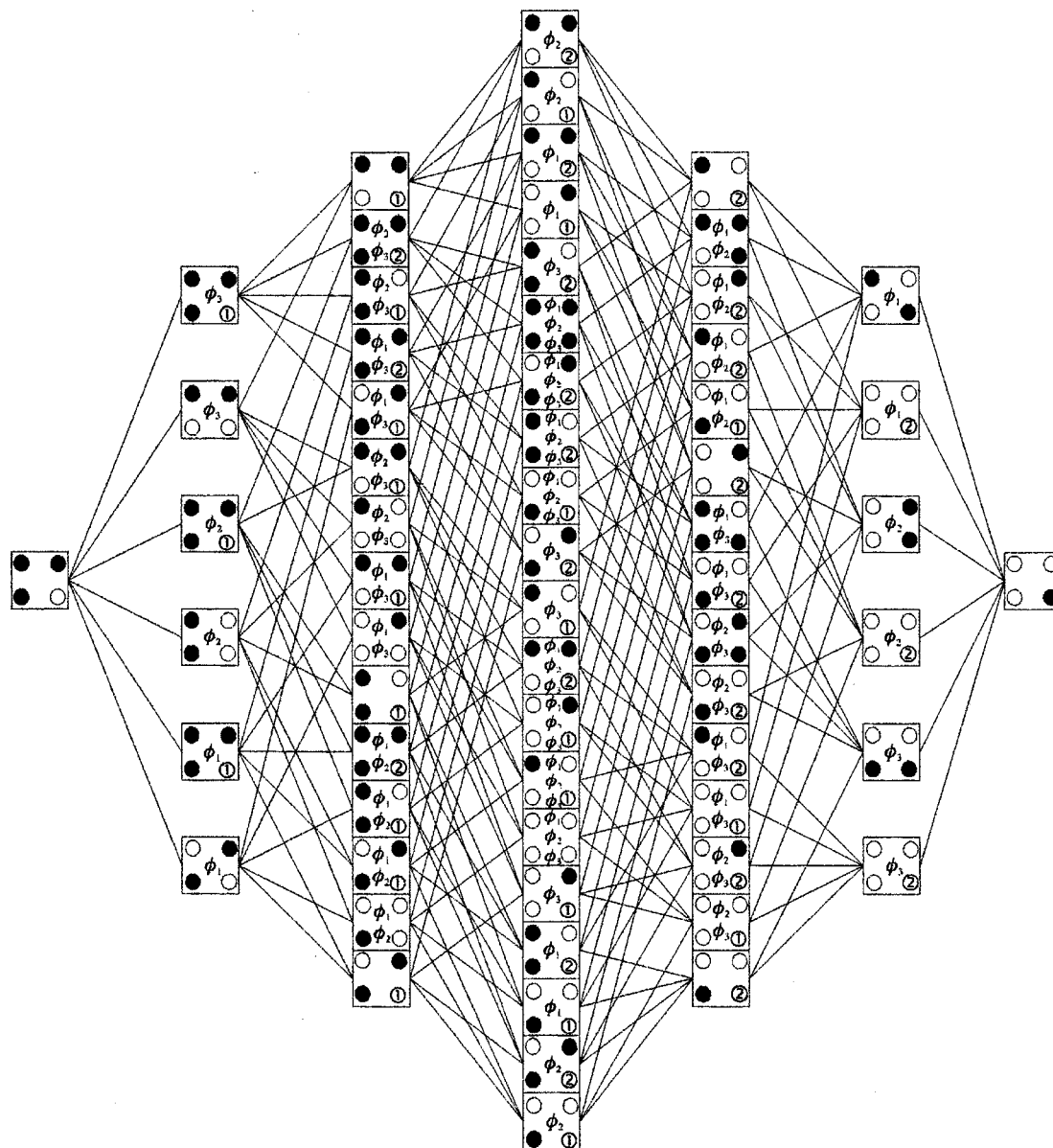


FIG. 7. State sequence diagram for the cooperative mechanism for 4CET. Species represented in the boxes are ABDC (clockwise from the top-left). Notation additional to that introduced in Fig. 2: $\textcircled{1}$ and $\textcircled{2}$ represent first and second virtual matter states ($|\xi^{\text{v}}\rangle$ and $|\xi^{\text{v}'}\rangle$ in the main text) and ϕ_n serves as a virtual photon label. Each of the 720 paths from left to right carries the same information content as one time-ordered diagram. Note that the connectivity is identical to Fig. 6.

A. Cooperative 4CET

For the mechanism of *cooperative* four-center energy transfer, sketched in Fig. 5(a), the blueprint of Fig. 6 is used as a guide in construction of the state-sequence diagram shown in Fig. 7. Each of the 720 paths through Fig. 7 is equivalent to a single time-ordered diagram of the conventional method. It is obvious that the state-sequence approach offers substantial advantages over conventional techniques in its conciseness; it also considerably expedites the quantum amplitude derivation.

By reading the matter and radiation states from the system state boxes in Fig. 7 (see the legend) the pertinent information may be extracted and deployed in the sixth order

perturbation term of Eq. (3.2). The summation over virtual states is accomplished by adding the contribution from each path traced across Fig. 7. Calculation of the quantum amplitude for *coop* four-center energy transfer (or any other type) is a lengthy process. Concisely, the procedure involves the identification and summation of numerous partial fractions, the conversion of virtual photon wave vector sums to a three-dimensional (3D) continuous integral, the use of tensor calculus to effect each polarization sum and subsequent solution of the resulting integral by the Residue Theorem. The methods mirror those used in the much simpler RET process—see for example Refs. 34, 45, 48 and 62. Following this procedure, the quantum amplitude results in a form which may be written as

$$M_{fi}^{coop} = \mu_i^{0\alpha(A)} V_{ij} \left(\frac{E_{\alpha 0}^A}{\hbar c}, \mathbf{R}_{DA} \right) \mu_k^{0\beta(B)} V_{kl} \left(\frac{E_{\beta 0}^B}{\hbar c}, \mathbf{R}_{DB} \right) \times \mu_m^{0\gamma(C)} V_{mn} \left(\frac{E_{\gamma 0}^C}{\hbar c}, \mathbf{R}_{DC} \right) \beta_{jln}^{\delta 0(D)}. \quad (3.9)$$

Equation (3.9) introduces two properties of the chromophore ξ . One is the transition dipole moment $\mu^{\xi r_0^1 \xi r_0^1(\xi)}$, of the general form,

$$\beta_{ijk}^{\xi r_0^1 \xi r_0^1(\xi)}(E^{(1)}, E^{(2)}, E^{(3)}) = \sum_{x,x'} \left\{ \frac{\mu_i^{\xi r_0^1 6x'} \mu_j^{x'x} \mu_k^{x\xi r_0^1}}{(E_{\xi r_0^1}^{\xi} + E^{(3)})(E_{\xi r_0^1}^{\xi} + E^{(2)} + E^{(3)})} + \frac{\mu_i^{\xi r_0^1 6x'} \mu_k^{x'x} \mu_j^{x\xi r_0^1}}{(E_{\xi r_0^1}^{\xi} + E^{(2)})(E_{\xi r_0^1}^{\xi} + E^{(2)} + E^{(3)})} \right. \\ + \frac{\mu_j^{\xi r_0^1 6x'} \mu_i^{x'x} \mu_k^{x\xi r_0^1}}{(E_{\xi r_0^1}^{\xi} + E^{(3)})(E_{1x'}^{\xi} + E^{(1)} + E^{(3)})} + \frac{\mu_j^{\xi r_0^1 6x'} \mu_k^{x'x} \mu_i^{x\xi r_0^1}}{(E_{\xi r_0^1}^{\xi} + E^{(1)})(E_{\xi r_0^1}^{\xi} + E^{(1)} + E^{(3)})} \\ \left. + \frac{\mu_k^{\xi r_0^1 6x'} \mu_i^{x'x} \mu_j^{x\xi r_0^1}}{(E_{\xi r_0^1}^{\xi} + E^{(2)})(E_{\xi r_0^1}^{\xi} + E^{(1)} + E^{(2)})} + \frac{\mu_k^{\xi r_0^1 6x'} \mu_j^{x'x} \mu_i^{x\xi r_0^1}}{(E_{\xi r_0^1}^{\xi} + E^{(1)})(E_{\xi r_0^1}^{\xi} + E^{(1)} + E^{(2)})} \right\}, \quad (3.11)$$

with the species in question accessing virtual matter states $|\xi^x\rangle$ and $|\xi^{x'}\rangle$. Furthermore the argument on the left and denominators on the right of (3.11) contain energy factors cast in the energy difference notation;

$$E_{\xi r_0^1 \xi r_0^1}^{\xi} = E_{\xi r_0^1}^{\xi} - E_{\xi r_0^1}^{\xi}, \quad (3.12)$$

along with energy terms specific to each relevant mechanism, $E^{(n)}$, exact expressions for which are given in Table II. Finally the energy conservation identity,

$$E_{\alpha 0}^A + E_{\beta 0}^B + E_{\gamma 0}^C = E_{\delta 0}^D = \hbar ck, \quad (3.13)$$

allows proper interpretation of the energy denominator data included in Table II.

Also introduced in Eq. (3.9) are three fully retarded, index-symmetric electric-dipole–electric-dipole interaction-pair tensors which can be written in universal form as

$$V_{ij}(p, \mathbf{R}_{\xi\xi'}) = \frac{e^{ipR_{\xi\xi'}}}{4\pi\epsilon_0 R_{\xi\xi'}^3} \{ (1 - ipR_{\xi\xi'}) \times [\delta_{ij} - 3(\hat{R}_{\xi\xi'})_i(\hat{R}_{\xi\xi'})_j] - (pR_{\xi\xi'})^2 \times [\delta_{ij} - (\hat{R}_{\xi\xi'})_i(\hat{R}_{\xi\xi'})_j] \}. \quad (3.14)$$

TABLE II. Energy factors for three-photon interaction tensors involved in 4CET.

	$E^{(1)}$	$E^{(2)}$	$E^{(3)}$
$\beta^{0\alpha(A)}$	$-\hbar ck$	$E_{\beta 0}^B$	$E_{\gamma 0}^C$
$\beta^{0\beta(B)}$	$-\hbar ck$	$E_{\alpha 0}^A$	$E_{\gamma 0}^C$
$\beta^{0\gamma(C)}$	$-\hbar ck$	$E_{\alpha 0}^A$	$E_{\beta 0}^B$
$\beta^{\delta 0(D)}$	$E_{\alpha 0}^A$	$E_{\beta 0}^B$	$E_{\gamma 0}^C$

$$\mu^{\xi r_0^1 \xi r_0^1(\xi)} \equiv \langle \xi r_0^1 | \mu^{(\xi)} | \xi r_0^1 \rangle. \quad (3.10)$$

Where three radiation–matter interactions occur at a single species, as above at the trap D, a three-photon interaction tensor $\beta^{\xi r_0^1 \xi r_0^1(\xi)}$ is also generated. The presence of such a factor was foreshown by the interaction-pairs describing the *coop* mechanism (AD BD CD) containing three occurrences of D. Such tensors govern the form of any three-photon interaction and take an explicit “hyperpolarizability” form expressible as

Equation (3.14) exhibits the physical properties associated with transfer of energy $\hbar cp$ between the interaction-pair $\xi\xi'$ with a mutual displacement vector;

$$\mathbf{R}_{\xi\xi'} = \mathbf{R}_{\xi} - \mathbf{R}_{\xi'}. \quad (3.15)$$

In viewing (3.14) as controlling the energy migration between the interaction-pair, the unification in the QED theory of resonance energy transfer is evident. The short- and long-range limits of $V_{ij}(p, \mathbf{R}_{\xi\xi'})$, when $pR_{\xi\xi'} \ll 1$ and $pR_{\xi\xi'} \gg 1$, respectively, accommodate both the Förster-type ($R_{\xi\xi'}^{-3}$ dependence) and radiative ($R_{\xi\xi'}^{-1}$ dependence) transfer.³²

B. Cooperative/accretive 4CET

Alongside the result of *coop* four-center energy transfer, the category of *coop/acc* mechanisms [the interaction-pairs BA CA AD, depicted in Fig. 5(c)] is also cast in terms of hyperpolarizabilities exemplified by Eq. (3.11). The three interactions occur at species A, and the quantum amplitude is given by

$$M_{fi}^{coop/acc1} = \mu_j^{\delta 0(D)} V_{ij} \left(\frac{E_{\delta 0}^D}{\hbar c}, \mathbf{R}_{DA} \right) \mu_k^{0\beta(B)} V_{kl} \left(\frac{E_{\beta 0}^B}{\hbar c}, \mathbf{R}_{AB} \right) \times \mu_m^{0\gamma(C)} V_{mn} \left(\frac{E_{\gamma 0}^C}{\hbar c}, \mathbf{R}_{AC} \right) \beta_{ilm}^{0\alpha(A)}, \quad (3.16)$$

where the exact form of $\beta_{ilm}^{0\alpha(A)}$ is given by (3.10) in conjunction with the information in Table II. The second and third *coop/acc* pathways can be generated by permuting A, B and C in (3.16). Note that such permutation entails not only interchanging species labels but also the designations of the associated excited states, relaxation energies and interspecies vectors, paying particular heed to the sets of interaction-pairs

TABLE III. Energy factors for two-photon interaction tensors involved in individual categories and mechanisms (Cat. Mech.). In each case such a tensor describes the behavior of two species (M1 and M2). Interaction-pairs (IP's) are shown explicitly to emphasize that the notation echoes the tensor form (see the main text).

Cat. Mech.	IP's	M1	$E^{(4)}$	$E^{(5)}$	M2	$E^{(4)}$	$E^{(5)}$
<i>acc/coop</i> 1	AD BC CD	D	$E_{0\beta}^B + E_{0\gamma}^C$	$E_{0\alpha}^A$	C	$-E_{0\beta}^B - E_{0\gamma}^C$	$E_{0\beta}^B$
2	AD CB BD	D	$E_{0\beta}^B + E_{0\gamma}^C$	$E_{0\alpha}^A$	B	$-E_{0\beta}^B - E_{0\gamma}^C$	$E_{0\gamma}^C$
3	BD AC CD	D	$E_{0\alpha}^A + E_{0\gamma}^C$	$E_{0\beta}^B$	C	$-E_{0\alpha}^A - E_{0\gamma}^C$	$E_{0\alpha}^A$
4	BD CA AD	D	$E_{0\alpha}^A + E_{0\gamma}^C$	$E_{0\beta}^B$	A	$-E_{0\alpha}^A - E_{0\gamma}^C$	$E_{0\gamma}^C$
5	CD AB BD	D	$E_{0\alpha}^A + E_{0\beta}^B$	$E_{0\gamma}^C$	B	$-E_{0\alpha}^A - E_{0\beta}^B$	$E_{0\alpha}^A$
6	CD BA AD	D	$E_{0\alpha}^A + E_{0\beta}^B$	$E_{0\gamma}^C$	A	$-E_{0\alpha}^A - E_{0\beta}^B$	$E_{0\beta}^B$
<i>acc</i> 1	AB BC CD	B	$-E_{0\alpha}^A - E_{0\beta}^B$	$E_{0\alpha}^A$	C	$E_{\delta 0}^D$	$E_{0\gamma}^C - E_{\delta 0}^D$
2	CB BA AD	B	$-E_{0\gamma}^C - E_{0\beta}^B$	$E_{0\gamma}^C$	A	$E_{\delta 0}^D$	$E_{0\alpha}^A - E_{\delta 0}^D$
3	AC CB BD	C	$-E_{0\alpha}^A - E_{0\gamma}^C$	$E_{0\alpha}^A$	B	$E_{\delta 0}^D$	$E_{0\beta}^B - E_{\delta 0}^D$
4	CA AB BD	A	$-E_{0\gamma}^C - E_{0\alpha}^A$	$E_{0\gamma}^C$	B	$E_{\delta 0}^D$	$E_{0\beta}^B - E_{\delta 0}^D$
5	BC CA AD	C	$-E_{0\beta}^B - E_{0\gamma}^C$	$E_{0\beta}^B$	A	$E_{\delta 0}^D$	$E_{0\alpha}^A - E_{\delta 0}^D$
6	BA AC CD	A	$-E_{0\beta}^B - E_{0\alpha}^A$	$E_{0\beta}^B$	C	$E_{\delta 0}^D$	$E_{0\gamma}^C - E_{\delta 0}^D$

involved in each pathway. For example the quantum amplitude for a second *coop/acc* pathway, where donor B undergoes the three-photon transition, is given by

$$M_{fi}^{coop/acc2} = \mu_i^{0\alpha(A)} V_{ik} \left(\frac{E_{\alpha 0}^A}{\hbar c}, \mathbf{R}_{BA} \right) \mu_l^{\delta 0(D)} V_{jl} \left(\frac{E_{\delta 0}^D}{\hbar c}, \mathbf{R}_{DB} \right) \\ \times \mu_m^{0\gamma(C)} V_{mn} \left(\frac{E_{\gamma 0}^C}{\hbar c}, \mathbf{R}_{CB} \right) \beta_{ijn}^{0\beta(B)}. \quad (3.17)$$

In (3.17) the relevant substitutions into the matter tensors and the energy transfer tensor arguments have been made. These account for the implications of the mechanism comprising interaction-pairs AB CB BD.

C. Accretive 4CET

In addition to categories comprising mechanisms whose quantum amplitudes are governed by ‘‘hyperpolarizabilities,’’ are those dependent upon another type of tensor. In mechanisms where two virtual photon interactions occur at any species behavior is described by a ‘‘polarizability.’’ First, take the *acc* mechanism (AB BC CD) depicted in Fig. 5(d), which yields the quantum amplitude

$$M_{fi}^{acc1} = \mu_i^{0\alpha(A)} V_{ij} \left(\frac{E_{0\alpha}^A}{\hbar c}, \mathbf{R}_{BA} \right) \alpha_{jk}^{0\beta(B)} \\ \times (-E_{0\alpha}^A - E_{0\beta}^B, E_{0\alpha}^A) V_{kl} \left(\frac{E_{0\alpha}^A + E_{0\beta}^B}{\hbar c}, \mathbf{R}_{CB} \right), \\ \times \alpha_{lm}^{0\gamma(C)} (E_{\delta 0}^D, E_{0\gamma}^C - E_{\delta 0}^D) V_{mn} \\ \times \left(\frac{E_{\delta 0}^D}{\hbar c}, \mathbf{R}_{DC} \right) \mu_i^{\delta 0(D)}. \quad (3.18)$$

Equation (3.18) features two examples of the generalized polarizability:

$$\alpha_{ij}^{\xi r_1 \xi r_0 (\xi)} (\pm E^{(4)}, \pm E^{(5)}) = \sum_x \frac{\mu_i^{\xi r_1 6x} \mu_j^{x \xi r_0}}{E_{\xi r_1 0x}^{\xi} \pm E^{(4)}} + \frac{\mu_j^{\xi r_1 6x} \mu_i^{x \xi r_0}}{E_{\xi r_1 0x}^{\xi} \pm E^{(5)}}, \quad (3.19)$$

with the signs of energy terms in the argument and denominator following the convention introduced for hyperpolariz-

abilities. The further five *acc* mechanisms are generated by permutation of A, B and C in Eq. (3.18). All ‘‘polarizabilities’’ in this category contain one positive and one negative argument term, reflecting the nature of energy input and output described by the tensor. Each *acc* four-center energy transfer mechanism involves excitation movement akin to single-photon scattering processes, as opposed to two-photon absorption or emission. For example, in Eq. (3.18) the scattering-like polarizability $\alpha_{jk}^{0\beta(B)} (-E_{0\alpha}^A - E_{0\beta}^B, E_{0\alpha}^A)$ connects two interaction-pairs AB and BC, with B adopting the role of a *bridge* (as seen in bichromophore and multichromophore arrays).^{8–11}

D. Accretive/cooperative 4CET

The final category of four-center energy transfer (*acc/coop*) contains both accretive and cooperative facets, similar to that described in Sec. III B. We recognize an analog of accretive channelling between donors occurring simultaneously with a cooperative interaction centred on the trap, hence *acc/coop*. Figure 5(b) (with interaction-pairs BC CD AD) engenders the matrix element;

$$M_{fi}^{acc/coop1} = \mu_i^{0\alpha(A)} V_{ij} \left(\frac{E_{0\alpha}^A}{\hbar c}, \mathbf{R}_{DA} \right) \\ \times \alpha_{jn}^{\delta 0(D)} (E_{0\beta}^B + E_{0\gamma}^C, E_{0\alpha}^A) V_{kl} \left(\frac{E_{0\beta}^B}{\hbar c}, \mathbf{R}_{BC} \right) \\ \times \alpha_{jk}^{0\gamma(C)} (-E_{0\beta}^B - E_{0\gamma}^C, E_{0\beta}^B) V_{mn} \\ \times \left(\frac{E_{0\beta}^B + E_{0\gamma}^C}{\hbar c}, \mathbf{R}_{DC} \right) \mu_k^{0\beta(B)}, \quad (3.20)$$

where $\alpha_{jn}^{\delta 0(D)} (E_{0\beta}^B + E_{0\gamma}^C, E_{0\alpha}^A)$ is a two-photon absorption analogue of the general polarizability (3.19). The two interaction-pairs that are conjoined by D are AD and BD, with the acceptor D clearly exhibiting its properties as a trap. A full set of polarizability denominator energies, revealing the precise forms of two-photon interaction tensors for each mechanism, is given in Table III.

E. Rate of 4CET

To conclude the calculation, the rate of four-center energy transfer Γ is determined by use of the Fermi Golden Rule:⁶⁶

$$\Gamma = \frac{2\pi}{\hbar} |M_{fi}^{4CET}| \rho_f, \quad (3.21)$$

where ρ_f is the density of states for the acceptor, determined by the vibronic structure of its excited state, and

$$M_{fi}^{4CET} = M_{fi}^{coop} + \sum_{j=1}^3 M_{fi}^{coop/accj} + \sum_{k=1}^6 M_{fi}^{acc/coopk} + \sum_{l=1}^6 M_{fi}^{accl}, \quad (3.22)$$

with representative examples of the amplitude constituents given by Eqs. (3.9), (3.16), (3.18), and (3.20). The remainder are generated from the data in Tables II and III, yielding the full quantum amplitude M_{fi}^{4CET} . Note that the rate contains 256 individual contributions, due to the squaring in (3.21). Explicitly these contributions comprise 16 diagonal terms, each relating to the square modulus of an individual pathway, and 240 off-diagonal terms which represent quantum interference between mechanisms. Pairing complex conjugate terms leaves a total of 136 distinct contributions to the rate. However, by recognizing the selection rules and symmetry associated with many real systems, the number of nonzero terms can be drastically reduced.

IV. SYMMETRY CONSIDERATIONS AND MECHANISTIC RESTRICTIONS

In the general theory of multiphoton interactions, group theory is a powerful tool. The use of simple symmetry arguments readily permits the determination of allowed transitions—see, for example, Ref. 67. Such methods have also proved invaluable in the analysis of multicenter transfer processes. For three-center energy transfer in ionic crystals, the validity of mechanistic pathways has been tested for specific lattice architectures using irreducible tensor calculus techniques.⁴⁰ In the following, four-center energy transfer systems will be shown to be equally amenable to appraisal in a similar manner. In the idealized dendrimeric structure depicted in Fig. 8, each dendron comprises a rank three Bethe lattice⁶⁸ of chemically and electronically identical donor units (termed A, where A is either A, B or C of the theory section) connected to an electronically and chemically distinct core species (the acceptor “trap” D). Assuming that all interconnecting bonds are equivalent and that the whole structure is planar, species D sits in a site of local symmetry described by the point group D_{3h} . We also assume that energy transfers only from the nearest neighbor donors A which sit in a C_{2v} site (higher generation species further out in the lattice occupying D_{3h} sites).

The group theoretical technique of irreducible Cartesian tensor analysis was borne out of excited state studies in multiphoton spectroscopy.^{69–71} Tensors of ranks one, two and three are manifest for both donor and trap species in the quantum amplitudes of 4CET systems—see Eqs. (3.9),

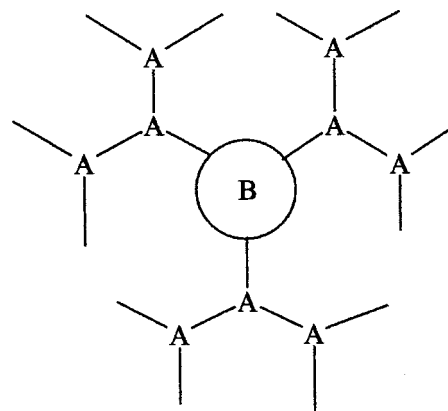


FIG. 8. Innermost structure of stylized, Bethe lattice-type dendrimer.

(3.16), (3.18), and (3.20). Each such tensor comprises sums of terms transforming as products of polar vector (transition electric dipole) components. Tensors of rank 2 and above may be represented in terms of sums of irreducible representations. For the general two-photon interaction tensor of (3.19) we may write the decomposition:⁴⁵

$$\alpha_{ij}^{\xi^r \xi^{r_0}(\xi)}(\pm E^{(4)}, \pm E^{(5)}) \equiv \alpha_{ij} = \alpha_{ij}^{(0+)} + \alpha_{ij}^{(1+)} + \alpha_{ij}^{(2+)}, \quad (4.1)$$

where the even-parity weight 0, 1 and 2 parts ($\alpha_{ij}^{(0+)}$, $\alpha_{ij}^{(1+)}$, and $\alpha_{ij}^{(2+)}$, respectively) transform under the full rotation-inversion group $O(3,r)$ ⁷² as a scalar, an antisymmetric pseudovector, and a traceless symmetric second-rank-tensor, respectively. Moreover, each term of weight j has $(2j+1)$ independent components.

Similarly the odd-parity three-photon interaction tensor (3.11) can be written as a sum of irreducible parts of weight 0 to 3 as⁷³

$$\beta_{ijk}^{\xi^r \xi^{r_0}(\xi)}(E^{(1)}, E^{(2)}, E^{(3)}) \equiv \beta_{ijk} = \beta_{ijk}^{(0-)} + \beta_{ijk}^{(1a-)} + \beta_{ijk}^{(1b-)} + \beta_{ijk}^{(1c-)} + \beta_{ijk}^{(2a-)} + \beta_{ijk}^{(2b-)} + \beta_{ijk}^{(3-)}. \quad (4.2)$$

Explicitly weight 0 transforms under the full rotation-inversion group $O(3,r)$ as a fully anti-symmetric pseudo-scalar; the three weight 1 contributions as polar vectors; the two weight 2 terms as traceless, index symmetric second-rank tensors; and the weight 3 as a traceless, fully index symmetric third-rank polar tensor. Each multiphoton transition to a state whose symmetry is referred to a given point group can be classified as either forbidden or allowed with regards to that symmetry. For any allowed multiphoton transition, it is necessary that the response tensor must possess at least one nonzero element. The criterion for this rule to be satisfied is that the product of the irreducible representations of the initial and final matter states of the chromophore must be spanned by one or more components of the tensor.⁷⁴

A. Implications for the acceptor

In the category of *coop* transfer the rank 3 tensor associated with the trap is totally index-symmetric, reducing its number of independent components and hence the number of

TABLE IV. Allowed tensor weight combinations in 4CET for trap species in a D_{3h} site. Rows correspond to excited state representations. In this notation, N^\pm denotes the tensor rank and parity followed by allowed weight combinations in parenthesis.

D_{3h}	<i>coop</i>	<i>acc/coop</i>	<i>coop/acc</i>	<i>acc</i>
A_1'	$3^-\{3\}$	$2^+\{02\}$	–	–
A_2'	$3^-\{3\}$	$2^+\{1\}$	–	–
E'	$3^-\{13\}$	$2^+\{2\}$	$1^-\{1\}$	$1^-\{1\}$
A_1''	–	–	–	–
A_2''	$3^-\{13\}$	–	$1^-\{1\}$	$1^-\{1\}$
E''	$3^-\{3\}$	$2^+\{12\}$	–	–

contributions to (4.2). The weight 0 and weight 2 terms contain full or partial contractions of β_{ijk} with a three-dimensional, antisymmetric Levi-Civita epsilon tensor, and hence vanish.⁶⁷ Thus the irreducible form of (3.11) is simply expressible as

$$\beta_{(ijk)} = \beta_{(ijk)}^{(1-)} + \beta_{(ijk)}^{(3-)}, \quad (4.3)$$

where the bracketed subscripts indicate index symmetry and $\beta_{(ijk)}^{(1-)}$ represents a sum of the weight 1 components in (4.2). As both weight 0 and weight 2 are zero for $\beta_{(ijk)}$, transitions from totally symmetric ground states to states of symmetry A_1'' are forbidden, as extensively discussed elsewhere.⁶⁷ All other transitions are allowed, as shown in Table IV.

For the *acc/coop* mechanism the acceptor response is controlled by a two-photon tensor that displays no index symmetry, as expressed by Eq. (4.1). Here trap transitions to states of symmetry A_1'' and A_2'' are forbidden by the selection rules. Finally in both the *coop/acc* and *acc* categories the acceptor undergoes a single photon interaction which results in its uptake of the total excitation energy within the system. As such, access to states of symmetry E' and A_2'' are allowed. Table IV shows the full irreducible representation combinations of allowed transitions for the trap in a D_{3h} site for each 4CET category.

B. Implications for the donors

In the *coop* mechanism the donor species undergo only single-photon transition dipole moment decay interactions—see Table V. Thus in the C_{2v} point group only transitions from states of symmetry A_2 are precluded—in the *coop* category, it is immediately obvious that this is the only controlling condition. For donor species participating in four-center energy transfer categories other than *coop*, determination of

TABLE V. Allowed tensor weight combinations in 4CET for donor species in a C_{2v} site. For categories other than *coop* both columns must have entries for a decay transition to be permissible between excited states of the given symmetry and a totally symmetric ground state.

C_{2v}	<i>coop</i>	<i>acc/coop</i>	<i>coop/acc</i>	<i>acc</i>
A_1	$1^-\{1\}$	$1^-\{1\}$	$2^+\{02\}$	$1^-\{1\}$ $3^-\{123\}$ $1^-\{1\}$ $2^+\{02\}$
A_2	–	–	$2^+\{12\}$	– $3^-\{023\}$ – $2^+\{12\}$
B_1	$1^-\{1\}$	$1^-\{1\}$	$2^+\{12\}$	$1^-\{1\}$ $3^-\{123\}$ $1^-\{1\}$ $2^+\{12\}$
B_2	$1^-\{1\}$	$1^-\{1\}$	$2^+\{12\}$	$1^-\{1\}$ $3^-\{123\}$ $1^-\{1\}$ $2^+\{12\}$

whether a transition is allowed or not is a little more complex as *two* criteria need to be simultaneously satisfied for a transition to be allowed.

In the *coop/acc* category the three-photon matter tensor displays *kl* index symmetry, reducing the total number of independent components from 27 to 18. The associated representation reduces as follows:

$$\beta_{i(kl)} = \beta_{i(kl)}^{(1\alpha-)} + \beta_{i(kl)}^{(1\beta-)} + \beta_{i(kl)}^{(2-)} + \beta_{i(kl)}^{(3-)}. \quad (4.4)$$

As can be seen from Table V, valid donor transitions must be both 1- and 3-photon allowed; the absence of a weight zero term in this case has little bearing on overall transition validity as access to all state symmetries in the C_{2v} point group are still permitted. Alongside Eq. (4.4) however, the behavior of the other two donors depends upon the single-photon transition dipole moment. Therefore the single-photon rules delineated for the *coop* category dominate the analysis, precluding only transitions to states of symmetry A_2 .

The two-photon tensors for donor species in 4CET exhibit no index symmetry, due to the difference in energy balance associated with the salient interactions. However, in the *acc/coop* and *acc* categories, not only is a nonzero weight 2^+ combination required to be allowed but also weight 1^- needs to be supported. This is due to different representatives of donor species A having to undergo both 1- and 2-photon transitions to facilitate the energy transfer in each category. (In a similar manner two donors undergo 1-photon transitions and a single donor a 3-photon transition in the *coop/acc* category.) Table V lists all pertinent allowed transition information for the donor species. In summary, even though transitions from A_2 states are both 2- and 3-photon allowed they are forbidden by all mechanisms because of the constraints of the 1-photon election rule

V. CONCLUSION

In this paper we have presented the different categories of four-center energy transfer and the individual mechanisms which can effect such a process. The quantum amplitudes of Eqs. (3.9), (3.16), (3.17), and (3.19), combined with the information in Tables II and III, allow full expression of the physics of 4CET. Tabulated energy denominator information can be used in conjunction with data from spectroscopic studies to suggest new synthetic routes toward multichromophore systems specifically designed to undergo 4CET. The group theory study undertaken at the end of the paper allows the prediction of valid transfer pathways for any given excited state symmetry of both the donor and acceptor species. In building suitably accommodating macromolecular systems, the excited and ground state symmetries of both donors and acceptors must be taken into account in order to secure a nonvanishing probability of energy transfer.

In the development of theory we have not explicitly entertained the possible effects of excitonic coupling and the delocalization of excitation between dendrimer branches. In the initial state of the four-center system at the heart of this work, all three donors are simultaneously excited and the lack of degeneracy means that the essential photophysics is correctly represented without regard to such issues. Similar remarks apply to our previous studies of three-center energy

transfer.^{36–40,42} Coupling and delocalization do however become significant when the number of participant donors exceeds the number of elementary excitations. For a triad of donors, Frenkel exciton formation is possible when one or two excitations are present; the role of such excitonic states on multicenter transfer is an avenue we are currently investigating⁷⁵—also see the other recent work on the exciton dynamics in such systems.^{76,77}

As a means of excited state relaxation, the concerted transfer of energy from all donors to the acceptor as per Eq. (2.3) is of course just one possibility. Indeed, 4CET may have to compete with a variety of donor decay processes according to the relative disposition of energy levels. To recognize the potential interplay of other decay routes recall that, for each four-center energy transfer path, nonenergy conserving virtual excited states are accommodated by the hyperpolarizabilities and polarizabilities, Eqs. (3.11) and (3.19), respectively. These states are generally associated with lifetimes which are immeasurably short, as determined by the principle of quantum uncertainty—but when suitably positioned in energy, such states can become significantly populated and exhibit measurable decay. With finite lifetimes for the intermediate states, stepwise rather than concerted transfer can ensue, affording opportunities for competing relaxation processes such as singlet–singlet annihilation. For example when intermediate donor excitations co-exist at donor species [as in the accretive mechanisms of Figs. 5(b), 5(c), 5(d)] singlet–singlet annihilation can quench immediate delivery of energy to the acceptor, energy levels permitting. The cooperative mechanism [Fig. 5(a)] however remains free from such competition.

In conclusion, the above theory offers a valid framework amenable to the representation and quantification of both concerted and stepwise excitation transfer in dendrimeric and multichromophore arrays. This, combined with the symmetry analysis, yields a framework within which to build such systems with the goal of observing the four-center energy transfer effect.

ACKNOWLEDGMENTS

The authors would like to thank the Engineering and Physical Sciences Research Council for a grant to support this work.

- ¹D. Kuciauskas, P. A. Liddell, S. Lin, T. E. Johnson, S. J. Weghorn, J. S. Lindsey, A. L. Moore, T. A. Moore, and D. Gust, *J. Am. Chem. Soc.* **121**, 8604 (1999).
- ²R. van Grondelle, J. P. Dekker, T. Gillbro, and V. Sundström, *Biochim. Biophys. Acta* **1187**, 1 (1994).
- ³S. Speiser, *J. Photochem.* **22**, 195 (1983).
- ⁴M. N. Berberan-Santos and B. Valeur, *J. Chem. Phys.* **95**, 8048 (1991).
- ⁵L. B.-Å. Johansson, P. Edman, and P.-O. Westlund, *J. Chem. Phys.* **105**, 10896 (1996).
- ⁶P. Edman, F. Bergström, and L. B.-Å. Johansson, *Phys. Chem. Chem. Phys.* **2**, 2795 (2000).
- ⁷B. Valeur, in *Fluorescent Biomolecules: Methodologies and Applications*, edited by D. M. Jameson and G. D. Reinhardt (Plenum, New York, 1989), pp. 269–303.
- ⁸S. A. Latt, H. T. Cheung, and E. R. Blout, *J. Am. Chem. Soc.* **87**, 995 (1965).
- ⁹R. D. Rauh, T. R. Evans, and P. A. Leermakers, *J. Am. Chem. Soc.* **90**, 6897 (1968).

- ¹⁰Y. Ren, Z. Wang, H. Zhu, S. J. Weininger, and W. G. McGimpsey, *J. Am. Chem. Soc.* **117**, 4367 (1995).
- ¹¹A. Harriman, M. Hissler, O. Trompette, and R. Ziessel, *J. Am. Chem. Soc.* **121**, 2516 (1999).
- ¹²M. N. Berberan-Santos, J. Pouget, B. Valeur, J. Canceill, L. Jullien, and J.-M. Lehn, *J. Phys. Chem.* **97**, 11376 (1993).
- ¹³R. K. Lammi, R. W. Wagner, A. Ambrose, J. R. Diers, D. F. Bocian, D. Holten, and J. S. Lindsey, *J. Phys. Chem. B* **105**, 5341 (2001).
- ¹⁴J. L. Sessler, V. L. Capuano, and A. Harriman, *J. Am. Chem. Soc.* **115**, 4618 (1993).
- ¹⁵P. G. Van Patten, A. P. Shreve, J. S. Lindsey, and R. J. Donohoe, *J. Phys. Chem. B* **102**, 4029 (1998).
- ¹⁶P. Brodard, S. Matzinger, E. Vauthey, O. Mongin, C. Papamicaël, and A. Gossauer, *J. Phys. Chem. A* **103**, 5858 (1999).
- ¹⁷L. Stryer, *Annu. Rev. Biochem.* **47**, 819 (1978).
- ¹⁸P. R. Selvin, in *Methods in Enzymology*, edited by K. Sauer (Academic, San Diego, 1995), Vol. 246, p. 300.
- ¹⁹B. Valeur, J. Mugnier, J. Pouget, J. Bouson, and F. Santi, *J. Phys. Chem.* **93**, 6073 (1989).
- ²⁰D. Vyprahčický, V. Pokorná, and F. Mikes, *Macromol. Chem. Phys.* **196**, 659 (1995).
- ²¹L. B.-Å. Johansson and J. Karolin, *Pure Appl. Chem.* **69**, 761 (1997).
- ²²F. Remacle, S. Speiser, and R. D. Levine, *J. Phys. Chem. B* **105**, 5589 (2001).
- ²³C. Devadoss, P. Bharathi, and J. S. Moore, *J. Am. Chem. Soc.* **118**, 9635 (1996).
- ²⁴D. M. Junge and D. V. McGrath, *Chem. Commun. (Cambridge)* **1997**, 857.
- ²⁵A. Archut and F. Vögtle, *Chem. Soc. Rev.* **27**, 233 (1998).
- ²⁶A. Andronov and J. M. J. Fréchet, *Chem. Commun. (Cambridge)* **2000**, 1701.
- ²⁷D.-L. Jiang and T. Aida, *Nature (London)* **388**, 454 (1997).
- ²⁸S. Encinas, A. M. Barthram, M. D. Ward, F. Barigelletti, and S. Campagna, *Chem. Commun. (Cambridge)* **2001**, 277.
- ²⁹D. L. Andrews and P. Allcock, *Chem. Soc. Rev.* **24**, 259 (1995).
- ³⁰D. L. Dexter, *J. Chem. Phys.* **21**, 836 (1953).
- ³¹G. D. Scholes and K. P. Ghiggino, *J. Chem. Phys.* **103**, 8873 (1995).
- ³²T. Förster, *Ann. Phys. (N.Y.)* **6**, 55 (1948).
- ³³J. S. Avery, *Proc. Phys. Soc. Jpn.* **88**, 1 (1966).
- ³⁴D. L. Andrews, *Chem. Phys.* **135**, 195 (1989).
- ³⁵R. P. Feynman, *Quantum Electrodynamics* (W. A. Benjamin, New York, 1962).
- ³⁶R. D. Jenkins and D. L. Andrews, *J. Phys. Chem. A* **102**, 10834 (1998).
- ³⁷R. D. Jenkins and D. L. Andrews, *Chem. Phys. Lett.* **301**, 235 (1999).
- ³⁸R. D. Jenkins and D. L. Andrews, *Phys. Chem. Chem. Phys.* **2**, 2837 (2000).
- ³⁹D. L. Andrews, *J. Raman Spectrosc.* **31**, 791 (2000).
- ⁴⁰D. L. Andrews and R. D. Jenkins, *J. Chem. Phys.* **114**, 1089 (2001).
- ⁴¹V. A. Morozov, *Russ. J. Phys. Chem.* **75**, 246 (2001).
- ⁴²D. L. Andrews and R. D. Jenkins, in *Complex Mediums II: Beyond Linear Isotropic Dielectrics*, edited by A. Lakhtakia, W. S. Weiglhofer, I. J. Hodgkinson, Proceedings of the SPIE (SPIE, Bellingham, WA, 2001), Vol. 4467, pp. 297–306.
- ⁴³V. A. Morozov, *Opt. Spectrosc.* **91**, 30 (2001).
- ⁴⁴G. D. Daniels and D. L. Andrews, *J. Chem. Phys.* **116**, 6701 (2002), preceding paper.
- ⁴⁵D. P. Craig and T. Thirunamachandran, *Molecular Quantum Electrodynamics* (Dover, New York, 1998).
- ⁴⁶J. Schwinger, *Phys. Rev.* **73**, 416 (1948).
- ⁴⁷R. P. Feynman, *Phys. Rev.* **76**, 769 (1949).
- ⁴⁸E. A. Power, *Introductory Quantum Electrodynamics* (Longmans, London, 1964).
- ⁴⁹W. E. Lamb and R. C. Retherford, *Phys. Rev.* **72**, 241 (1947).
- ⁵⁰H. B. G. Casimir, *Proc. K. Ned. Akad. Wet.* **B51**, 793 (1948).
- ⁵¹S. K. Lamoreaux, *Phys. Rev. Lett.* **78**, 5 (1997); **81**, 5475 (1998).
- ⁵²D. L. Andrews and L. C. Dávila Romero, *Eur. J. Phys.* **22**, 447 (2001).
- ⁵³E. A. Power, *Am. J. Phys.* **34**, 516 (1966).
- ⁵⁴E. A. Power and T. Thirunamachandran, *Phys. Rev. A* **28**, 2649 (1983).
- ⁵⁵E. A. Power and T. Thirunamachandran, *Phys. Rev. A* **28**, 2663 (1983).
- ⁵⁶E. A. Power and T. Thirunamachandran, *Phys. Rev. A* **28**, 2671 (1983).
- ⁵⁷E. A. Power and S. Zienau, *Philos. Trans. R. Soc. London, Ser. A* **251**, 427 (1959).
- ⁵⁸J. Knoester and S. Mukamel, *Phys. Rev. A* **40**, 7065 (1989).
- ⁵⁹G. Juzeliūnas and D. L. Andrews, *Phys. Rev. B* **49**, 8751 (1994).

- ⁶⁰G. Juzeliūnas and D. L. Andrews, *Phys. Rev. B* **50**, 13371 (1994).
- ⁶¹P. W. Milloni, *J. Mod. Opt.* **42**, 1991 (1995).
- ⁶²G. Juzeliūnas and D. L. Andrews, in *Resonance Energy Transfer*, edited by D. L. Andrews and A. A. Demidov (Wiley, Chichester, 1999), pp. 65–107.
- ⁶³R. D. Jenkins, D. L. Andrews, and L. C. Dávila Romero, *J. Phys. B* **35**, 445 (2002).
- ⁶⁴D. L. Andrews, *Nonlinear Opt.* **8**, 25 (1994).
- ⁶⁵I. D. Hands, S. J. Lin, S. R. Meech, and D. L. Andrews, *Phys. Rev. A* **62**, 023807 (2000).
- ⁶⁶P. A. M. Dirac, *The Principles of Quantum Mechanics*, 4th ed. (Oxford University Press, New York, 1996).
- ⁶⁷D. L. Andrews, *Spectrochim. Acta, Part A* **46**, 871 (1990).
- ⁶⁸M. Kurata, R. Kikuchi, and T. Watari, *J. Chem. Phys.* **21**, 434 (1953).
- ⁶⁹J. Jerphagnon, *Phys. Rev. B* **2**, 1091 (1970).
- ⁷⁰D. L. Andrews and T. Thirunamachandran, *J. Chem. Phys.* **68**, 2941 (1978).
- ⁷¹D. L. Andrews and W. A. Ghoul, *Phys. Rev. A* **25**, 2647 (1978).
- ⁷²S. K. Kim, *Group Theoretical Methods and Applications to Molecules and Crystals* (Cambridge University Press, Cambridge, 1999).
- ⁷³D. L. Andrews and P. J. Wilkes, *J. Chem. Phys.* **83**, 2009 (1985).
- ⁷⁴S. F. A. Kettle, *Symmetry and Structure* (Wiley, New York, 1985).
- ⁷⁵R. D. Jenkins and D. L. Andrews (work in progress).
- ⁷⁶V. Čápek, I. Barvík, and P. Heřman, *Chem. Phys.* **270**, 141 (2001).
- ⁷⁷P. Heřman and I. Barvík, *Chem. Phys.* **274**, 199 (2001).